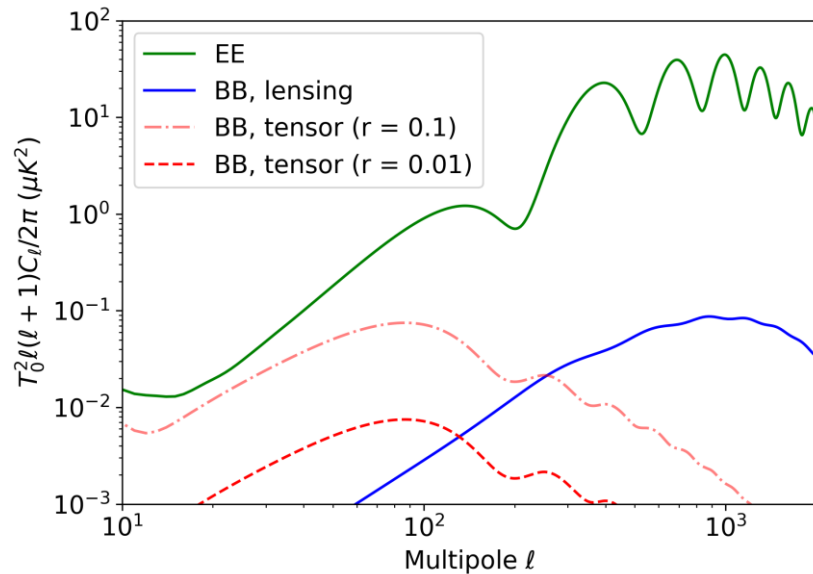
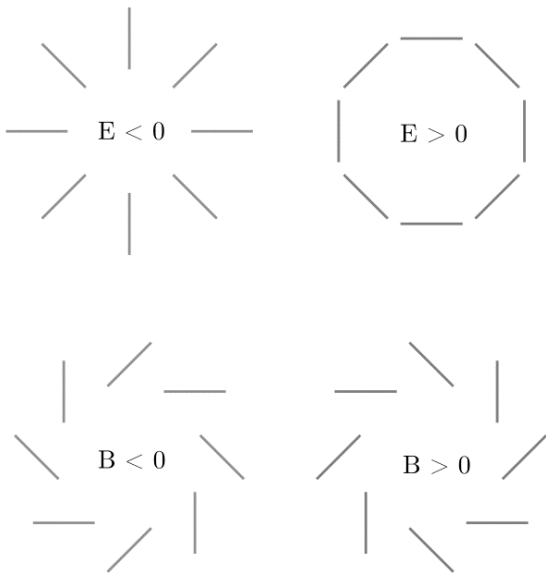



# Integrated Electrical Properties of the Cryogenic Readout System for POLARBEAR/Simons Array

Kayla Mitchell<sup>1</sup>, Darcy Barron<sup>1</sup>, John Groh, Kam Arnold, Tucker Elleflot, Logan Howe, Jennifer Ito, Adrian Lee, Lindsay Ng Lowry, Adam Anderson, Jessica Avva, and the POLARBEAR Collaboration

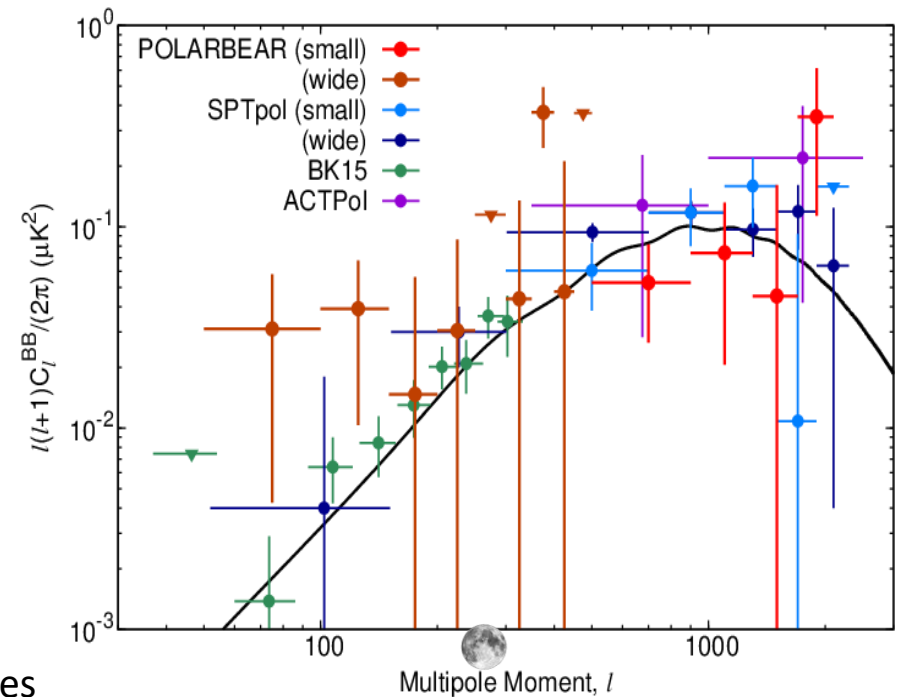
<sup>1</sup>University of New Mexico  
New Mexico Symposium  
2020



  $l \sim 400 = 0.5$  degrees

Illustrated here are cartoon versions of the CMB polarization patterns observed: curl-free E-modes and divergence-free B-modes.

Plotted here are autocorrelations of the expected amplitudes of CMB polarization signals. This is plotted against angular scale,  $l$ . Large angular distances correspond to smaller values of  $l$ . The amplitude of the inflationary signal depends on  $r$ , the energy scale of inflation.



This plot zooms in on the region with the peak from gravitational lensing, which has been detected by several experiments in the past 5 years. Only upper limits have been placed on the inflationary signal so far.

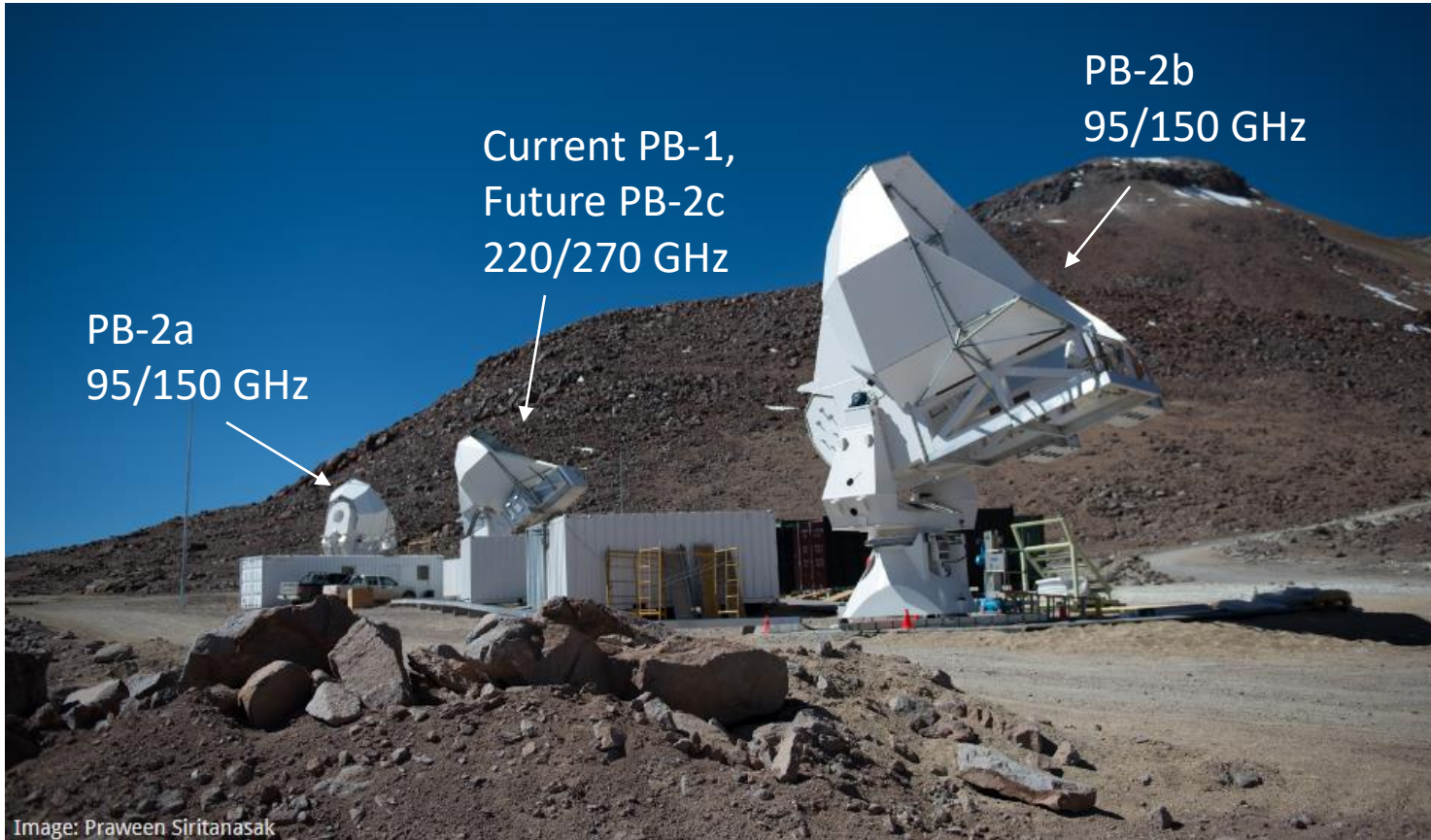


Image: Praween Siritanasak

# POLARBEAR / Simons Array

- The POLARBEAR / Simons Array is a dedicated CMB polarization instrument located in the Atacama Desert in Chile at an elevation of 5200m.
- A significant upgrade is being made from POLARBEAR-1 (1 telescope, 1 frequency) to POLARBEAR-2 with 3 telescopes, observing at 4 frequency bands (95/150/220/270 GHz).
- When completed, the array will have over 20,000 superconducting transition edge detectors cooled to 300 mK.



## UC Berkeley

Tylor Adkins  
Shawn Beckman  
Kevin Crowley  
John Groh  
Charles Hill  
William Holzapfel  
Oliver Jeong  
Adrian Lee  
Dick Plambeck  
Christopher Raum  
Paul Richards  
Benjamin Westbrook  
Yuyang Zhou



## UC San Diego

Kam Arnold  
David Boettger  
Bryce Bixler  
Nicholas Galitzki  
Jennifer Ito  
Brian Keating  
David Leon  
Lindsay Lowry  
Marty Navaroli  
Michael Randall  
Max Silva-Feaver  
Jake Spisak  
Grant Teply



## KEK

Tijmen de Haan  
Takaho Hamada  
Masaya Hasegawa  
Masashi Hazumi  
Daisuke Kaneko  
Yuto Minami  
Yuuko Segawa  
Junichi Suzuki  
Sayuri Takatori  
Daiki Tanabe



## U Tokyo

Yuji Chinone  
Akito Kusaka  
Haruki Nishino  
Kyohei Yamada



## SISSA

Carlo Baccigalupi  
Nicoletta  
Krachmalnicoff  
Anto Lonappan  
Davide Poletti



## Kyoto U.

Osamu Tajima  
Shunsuke Adachi  
Tomofumi Abe



## U Manchester

Mark McCulloch  
Lucio Piccirillo



## McGill University

Matt Dobbs  
Joshua Montgomery  
Graeme Smecher



## Católica (PUC)

Rolando Dunner



## Lawrence Berkeley NL

Julian Borrill  
Reijo Keskitalo  
Theodore Kisner  
Akito Kusaka  
Eric Linder  
Aritoki Suzuki  
Tucker Elleflot



## Laboratoire Astroparticule & Cosmologie

Hamza El Bouhargani  
Baptiste Jost  
Josquin Errard  
Radek Stompor  
Clara Vergès



## U of Sussex

Giulio Fabbian  
Julien Peloton



## Dalhousie

Scott Chapman  
Colin Ross  
Kaja Rotermund  
Alexei Tikhomirov



## U of Illinois at Urbana Champaign

Chang Feng



## Imperial College

Andrew Jaffe  
Daisy Mak



## Kavli IPMU

Nobuhiko Katayama  
Frederick Matsuda  
Tomotake Matsumura  
Satoru Takakura



## Cardiff University

Peter Ade



## CU Boulder

Nils Halverson  
Greg Jaehnig



## U. Melbourne

Christian Reichardt  
Federico Bianchini  
Anh Pham



## Stanford University

Dominic Beck



## U. New Mexico

Darcy Barron  
Kayla Mitchell



## Yokohama National U.

Takuro Fujino  
Haruaki Hirose  
Shuhei Kikuchi



## Argonne NL

Amy Bender

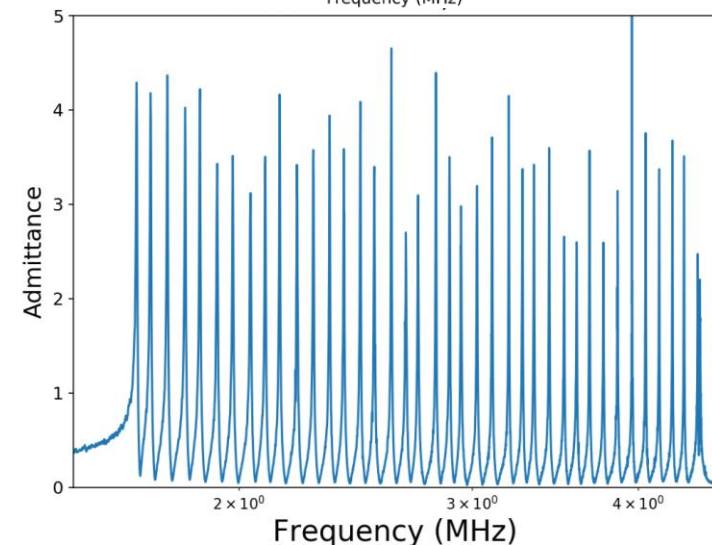
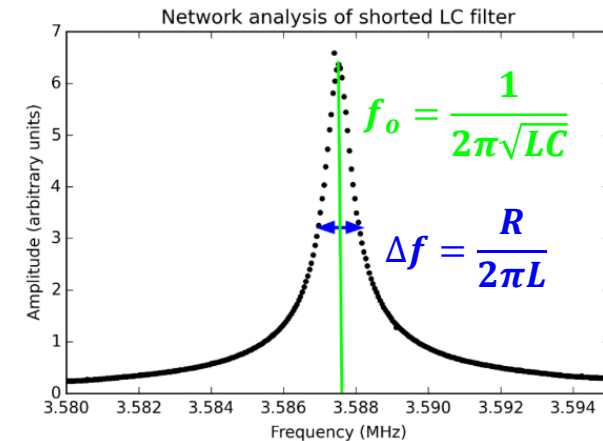
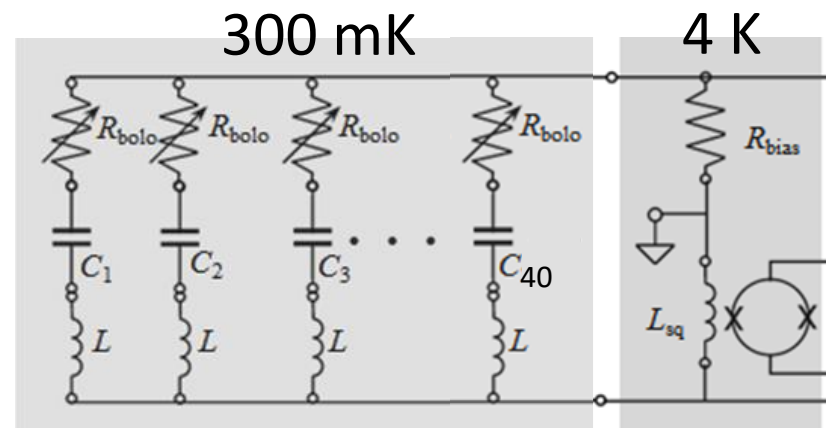


And many more in  
years past!



# Frequency-Division Multiplexed Readout for CMB Measurements

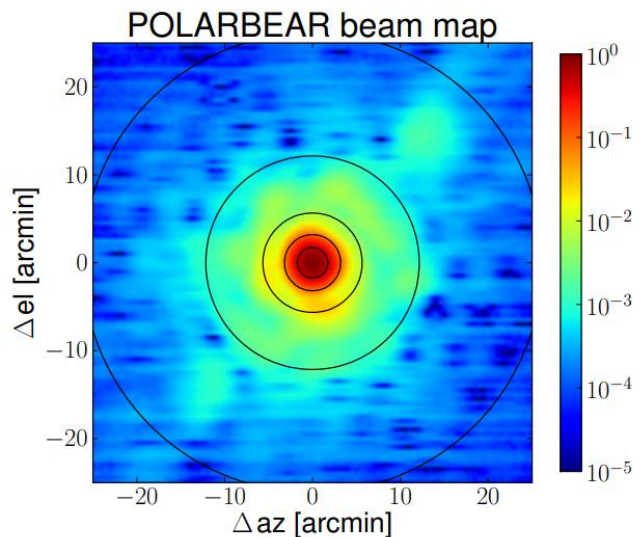
- Increasing sensitivity requires adding more detectors, and current experiments have thousands of transition edge sensors (TES).
- This requires multiplexing, where the signal from many detectors is read out on a single pair of wires, reducing thermal load, complexity, and cost.
  - Each transition edge sensor has a channel defined by an inductor and capacitor in series, forming an RLC resonant peak
  - The signal from optical power shows up as an amplitude modulation.
  - All tones are fed through a cold SQUID amplifier.
  - Signals are then demodulated with room temperature electronics ([Bandura et al. 2016](#))
- DfMux frequency-division multiplexing has been used in several CMB experiments ([Dobbs et al. 2012](#))
- Digital Active Nulling nulls current through SQUID with digital feedback loop at each detector frequency ([de Haan et al. 2012](#))



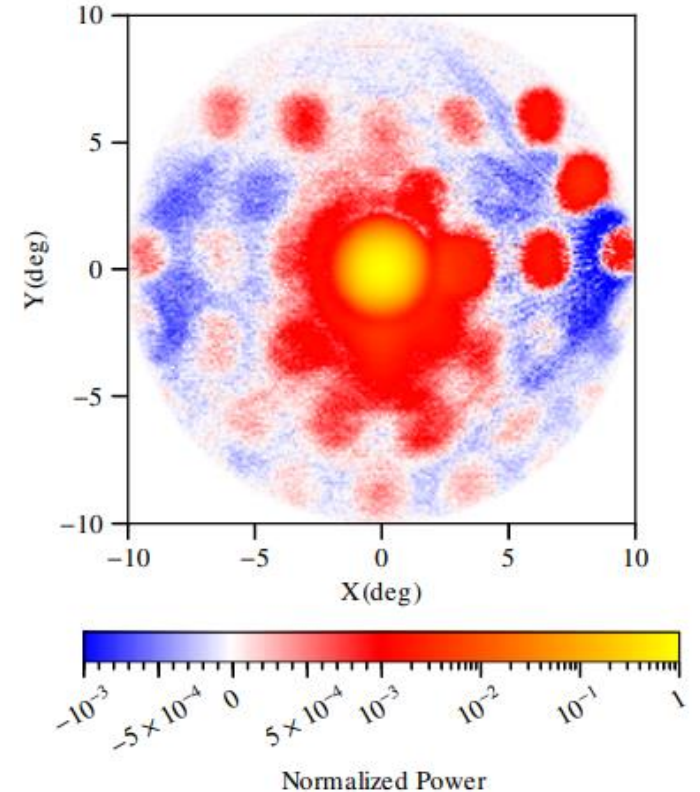


# Sources and effects of crosstalk

- Crosstalk between bolometers due to coupling from the multiplexed readout leads to leakage of polarization and temperature ([POLARBEAR Collab. 2014](#))
- Crosstalk is highest in channels that share the same SQUID in readout and are closest together in bias frequency ([Dobbs et al. 2012](#))
- We need to characterize and understand our levels of crosstalk to avoid unaccounted systematic errors



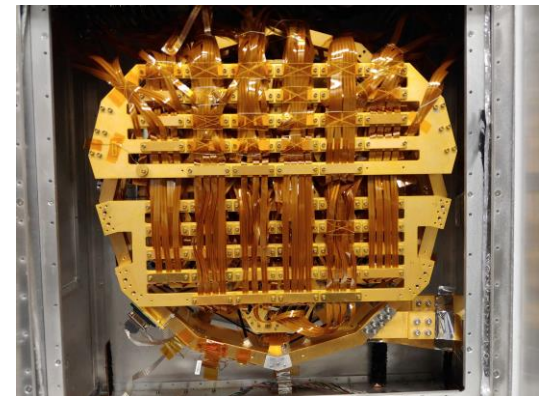
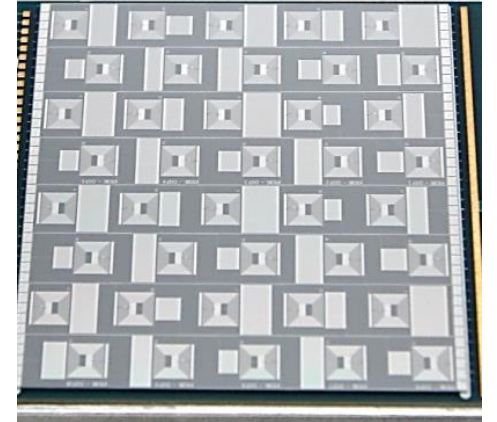
A map of Jupiter from 2 years of co-added PB-1 data with crosstalk levels of about 1% ([POLARBEAR Collab. 2014](#)). The sensitivity of PB-2 requires lower levels of crosstalk (for PB-1 1% was good enough, PB-2 will be more sensitive)



An example of crosstalk from the CLASS experiment observing the moon with images resembling the focal plane from electrical crosstalk and possible optical ghosting ([Xu et al. 2020](#)).

# Readout design for POLARBEAR-2/Simons Array

- Important developments for Next-Gen Dfmux (used in PB-2, SPT-3G)
  - Total readout bandwidth was greatly increased with development of Digital Active Nulling ([de Haan et al. 2012](#)).
  - Planar lithographed superconducting LC resonators increased precision of peak frequencies, and reduced loss at higher frequencies ([Rotermund et al. 2015](#)).
  - Low-inductance, low thermal conductivity superconducting NbTi striplines act as a thermal break while minimizing impedance in series with TES ([Avva et al. 2018](#)).
- These improvements led to a design for POLARBEAR-2 with a multiplexing factor of 40x, compared to 8x for POLARBEAR-1 ([Hattori et al. 2015](#))
  - Also demonstrated with 68x multiplexing in SPT-3G ([Bender et al. 2016](#))



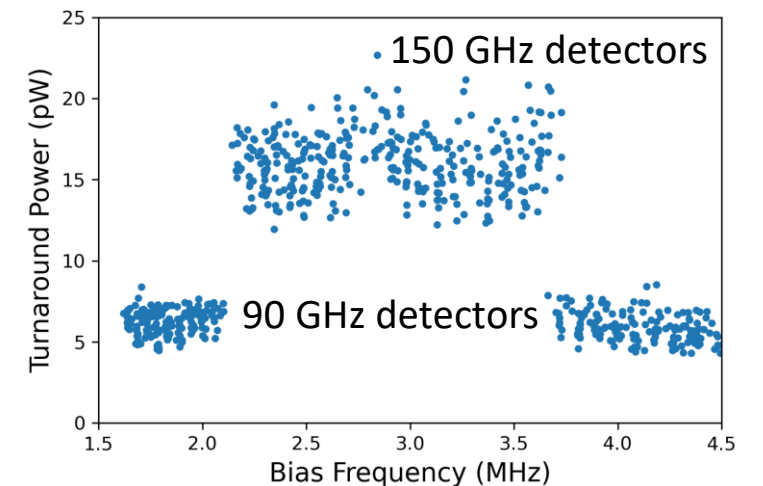
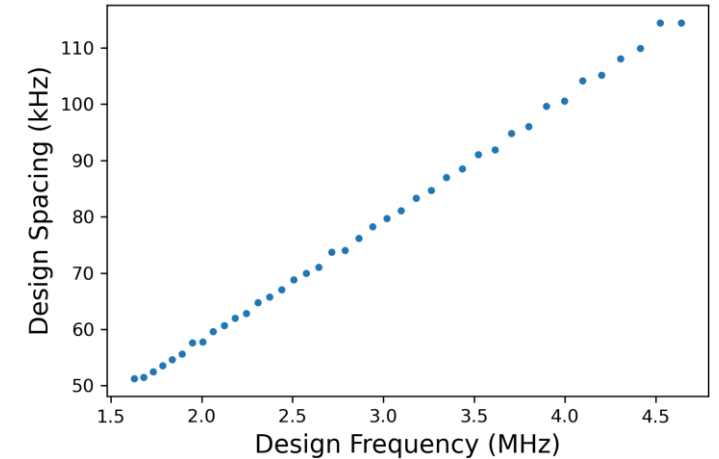


# Design parameters for POLARBEAR-2 Readout

The requirements on readout performance are related to noise, detector stability and linearity, and crosstalk.

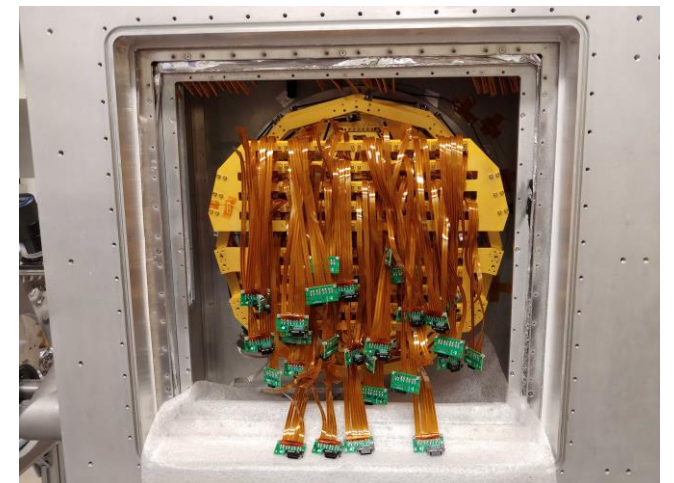
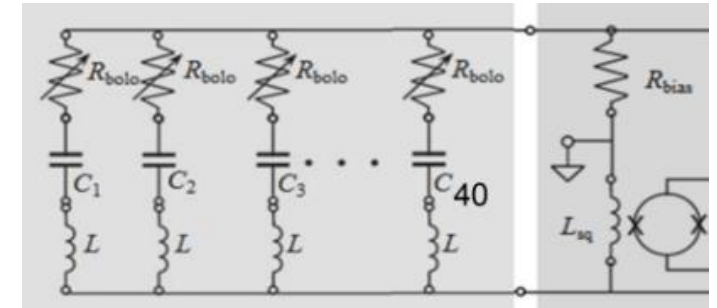
The multiplexing factor (channels per SQUID and pair of wires) is set by total bandwidth, peak bandwidth, and peak spacing.

- Total Readout bandwidth: 1.5 – 4.5 MHz
- Channel spacing: 50 kHz – 110 kHz
- Detector time constants: 1 - 5 ms
- Channel-defining inductor: 60  $\mu$ H
- Channel-defining capacitor: 21 – 161 pF
- Detector resistance: 1 Ohm
- Series resistance: 0.2 Ohms
- Series inductance: 60 nH
- SQUID input coil inductance: 50 nH



# Further design changes after POLARBEAR-2a

- After readout for POLARBEAR-2a was completed, minor design improvements were made for POLARBEAR-2b and POLARBEAR-2c.
  - The lithography mask was updated to make ordering of L-C-R components consistent.
    - A checkerboard pattern of alternating LC-CL was designed to minimize crosstalk from inductive coupling, but differences in series resistance were measured depending on electrical ordering.
    - A minor mask error causing the two highest peaks to be closer than designed was fixed at the same time.
  - The superconducting metal was switched from aluminum ( $T_c=1.2\text{K}$ ) to niobium ( $T_c=9\text{K}$ ).
    - No observed issues with Al when operating at base temperature, 300mK.
    - Some issues with testing and characterization above bolometer  $T_c$  and during fridge recycling ( $T \sim 0.8\text{-}1\text{K}$ ) were observed, as peaks shift due to kinetic inductance.
  - Consistent length NbTi striplines were implemented.
  - A damping resistor was added across the input coil to improve stability with lower input inductance SQUIDs.



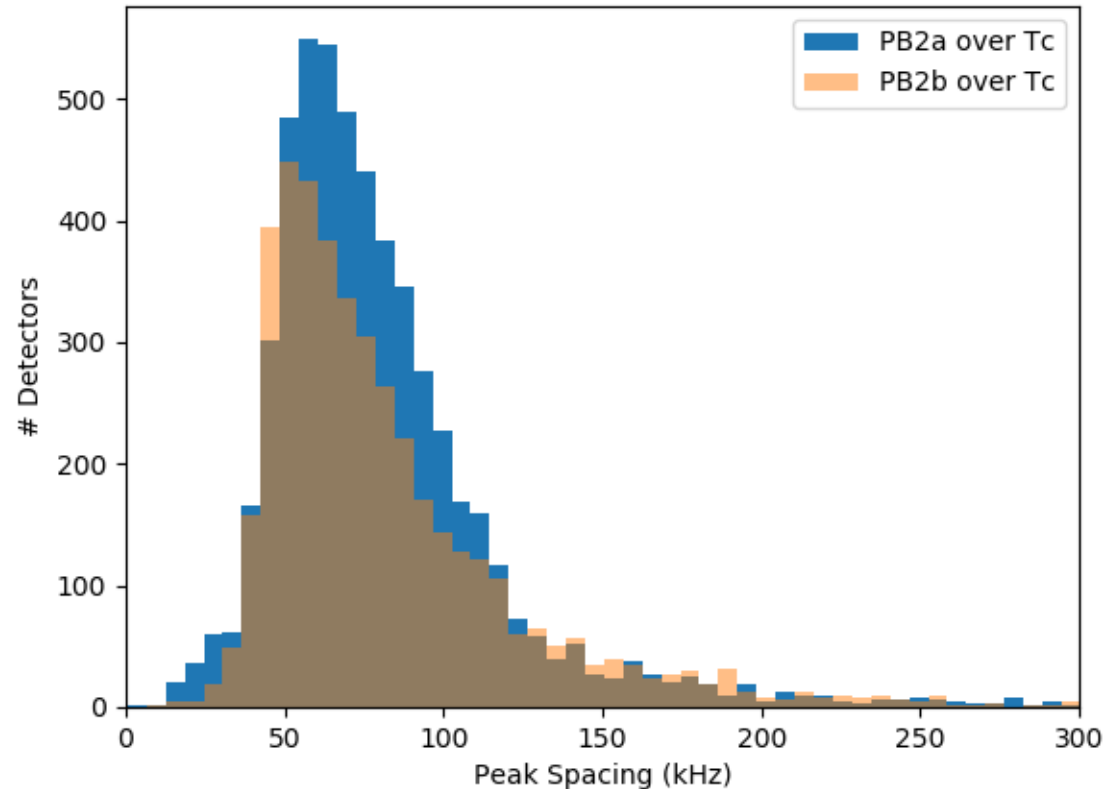
# Results: Measured integrated readout performance in POLARBEAR-2

Including comparisons between POLARBEAR-2a and POLARBEAR-2b

- Measured spacing between peaks
- FWHM of RLC peaks
- Expected crosstalk levels
- Measured parasitic resistance in series with detector



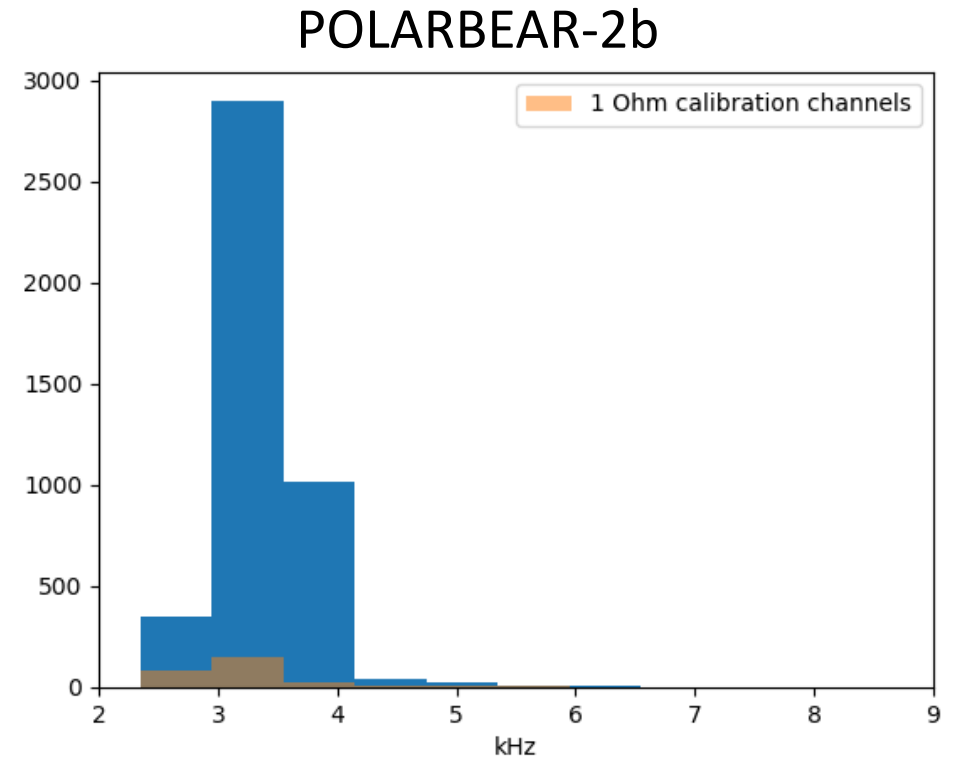
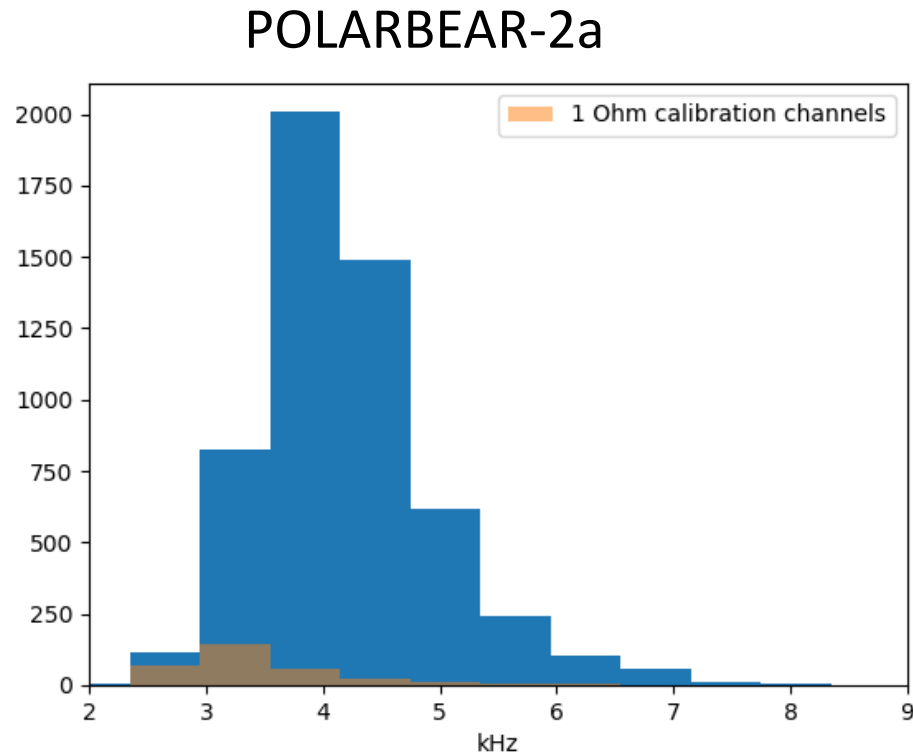
# Measured Peak Spacing for POLARBEAR-2



Some peak collisions are due to error in lithography mask for PB2a that placed two peaks closer than designed.

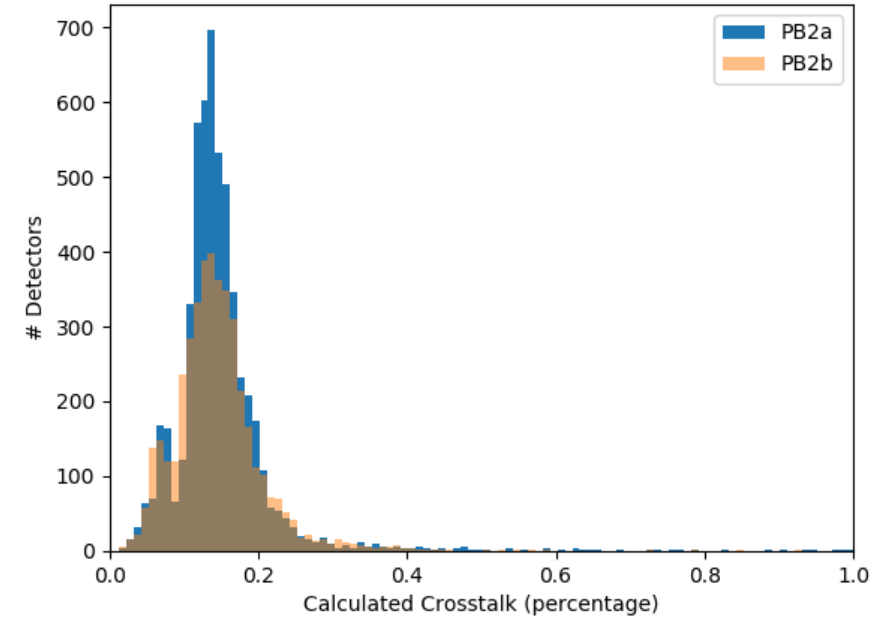
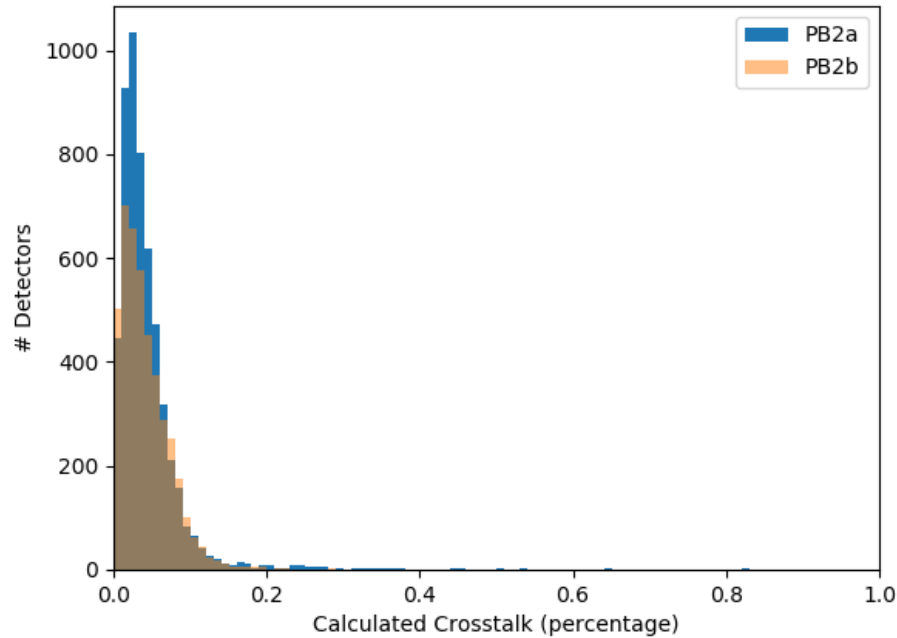
Calculated here is the distance between adjacent channel peaks identified in network analysis data for PB-2a and PB-2b. Peaks that scatter closer together will have higher levels of crosstalk. Large peak spacings are due to missing peaks.

# Measured FWHM for POLARBEAR-2 Channels



These histograms show the FWHM of admittance measured in a network analysis sweep with bolometers in their normal state, above the superconducting transition for PB-2a (left) and PB-2b (right). One-ohm calibration channels are highlighted.

# Calculated crosstalk from peak spacing for detectors above superconducting transition



$$\text{Crosstalk Ratio}_{\text{bias carrier leakage}} = \left( \frac{R_{\text{bolo}}}{4\pi L \Delta f} \right)^2$$

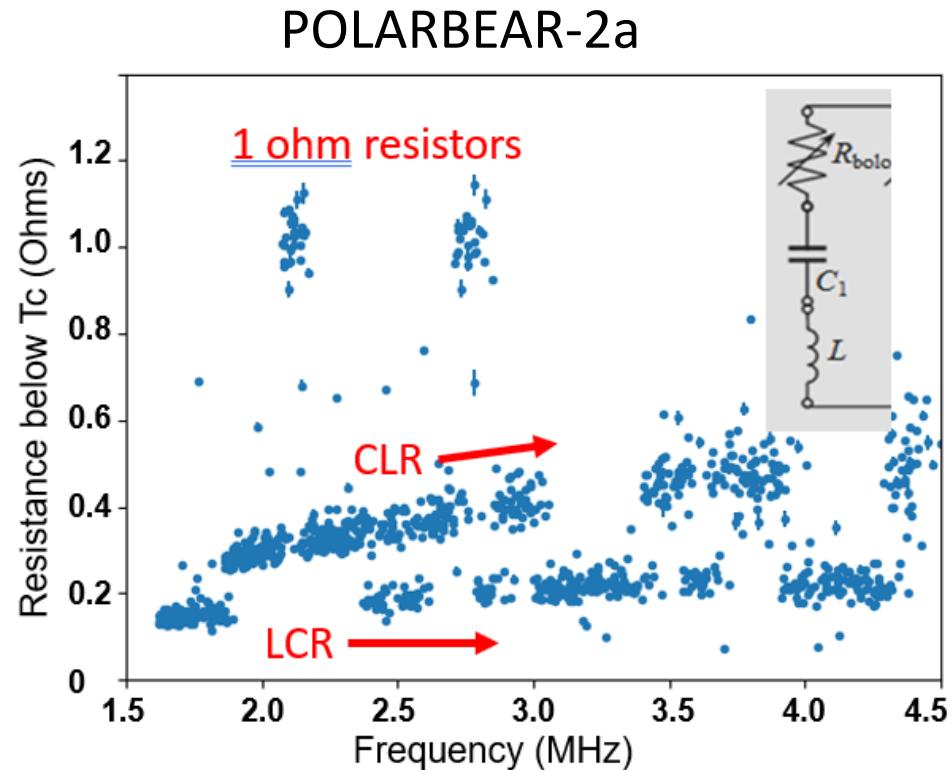
Above is the bias carrier leakage crosstalk magnitudes for PB-2a and PB-2b calculated using the distance between channel peaks, with  $R_{\text{bolo}} = 1 \text{ ohm}$ ,  $L = 60 \text{ } \mu\text{H}$ .

$$\text{Crosstalk Ratio}_{\text{non-zero impedance}} = - \frac{I_{\text{Ch}_{i\pm 1}}^{f_i}}{I_{\text{Ch}_i}^{f_i}} \frac{f_i}{\Delta f} \frac{L_{\text{stray}}}{L}$$

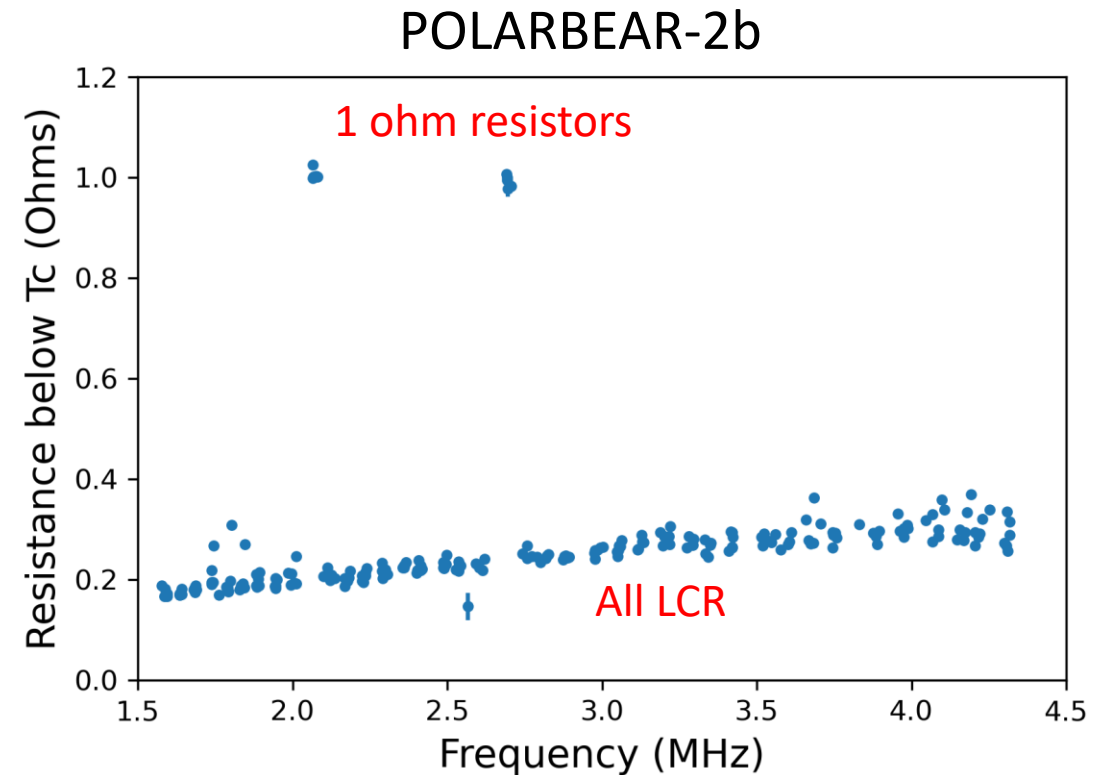
Above is the non-zero impedance crosstalk magnitudes for PB-2a and PB-2b calculated using the distance between channel peaks, with  $L_{\text{stray}} = 45 \text{ nH}$ ,  $L = 60 \text{ } \mu\text{H}$ .



# Measured parasitic resistance in series with detector



The measurements above were made for PB-2a, with detectors in their superconducting state in dark laboratory integration testing. Resistance is measured through  $V=IR$  one channel at a time, and fits to network analysis data are in agreement.



Above are the same measurements, for PB-2b, which has the LCR ordering now consistent, but adds a 20 ohm damping resistor in parallel with the comb, adding to the measured parasitic resistance.

# Notes on future work/current status

- POLARBEAR-2a had first light in January 2019.
  - Instrument characterization and analysis of data taken in the first year is ongoing.
- POLARBEAR-2b began assembly in Chile in March 2020.
- Progress was halted in March when the Chilean site was shut down due to the global impacts of COVID-19.
- Assembly and observations will resume when it is safe to travel to and work at the site.